THE PHYSICS OF STRONG COLOR FIELDS: NEW FRONTIER OF QCD*

Dmitri Kharzeev

Nuclear Theory Group, Brookhaven National Laboratory
Upton, New York 11973, USA

(Received November 16, 2006)

At high energies, the properties of hadronic and nuclear interactions are determined by the dynamics of strong color fields. The physics of strong color fields is responsible for many of the phenomena observed at RHIC and is expected to describe both pp and AA collisions at the LHC. These lectures are intended as an elementary introduction into QCD and its behavior in the strong field limit.

PACS numbers: 12.38.–t, 12.38.Mh, 24.85.+p, 25.75.Nq

1. Introduction

The Standard Model is a remarkably successful physical theory, but it leaves many questions unanswered. Many of them (*e.g.* the origin of fermion generations) concern the physics above the electroweak scale $\sim M_W, M_Z \sim$ 100 GeV and will soon be addressed experimentally at the LHC — a new high energy outpost of particle physics. Other, and no less important, open questions deal with the physics at the QCD scale, $\sim$ 1 GeV: what binds quarks and gluons together? what is the origin of hadron masses? In the decades following the advent of QCD it has become clear that the answers to these questions are buried deep and can be uncovered only through a detailed understanding of non-linear dynamics of gauge fields in this theory. Such an understanding can be gained through the study of gauge fields of varying intensity. Strong color fields, as will be discussed in these lectures, can be achieved in hadron and nuclear collisions at high energies.

In nuclear interactions, RHIC at BNL currently provides the highest available collision energy, up to 200 GeV per nucleon in the c.m.s. In hadron–hadron interactions, the record c.m.s. energy of about 2 TeV has been

* Presented at the XLVI Cracow School of Theoretical Physics, Zakopane, Poland May 27–June 5, 2006.

achieved at the Tevatron at Fermilab. Both of these records will soon fall with the emergence of the LHC at CERN, which will push the c.m.s. energy to 14 TeV in pp collisions and to 5.5 TeV per nucleon in nuclear collisions. We have every reason to expect a great improvement in our understanding of the foundations of our physical World!

Having a working theory of strong interactions is important for one simple reason — strong interaction is indeed the strongest force of Nature. It is responsible for over 80% of the baryon masses, and thus for most of the mass of everything on Earth and in the visible Universe. Strong interactions bind nucleons in nuclei which, being then dressed with electrons and bound into molecules by the much weaker electro-magnetic force, give rise to the entire variety of our world.

Quantum Chromodynamics (QCD) is *the* theory of strong interactions. The fundamental degrees of freedom of QCD, quarks and gluons, are already well established even though they cannot be observed as free particles, but only in color neutral bound states (confinement). Today, QCD has firmly occupied its place as part of the Standard Model. However, understanding the physical world does not only mean understanding its fundamental constituents; it means mostly understanding how these constituents interact and bring into existence the entire variety of physical objects composing the universe. In these lectures, we try to explain why high energy experiments with protons and nuclei offer us unique tools to study QCD.

I would like to emphasize that these lectures are intended as an elementary introduction for students just entering the field; the references are scarce, and I refer the interested reader to several reviews on the subject [1–4] as well as to the other lectures in this volume.

2. The theory of strong interactions: QCD

2.1. The foundations

So what is Quantum Chromo-Dynamics? QCD emerges when the naïve quark model is combined with local SU(3) gauge invariance. Quark model classifies the large number of hadrons in terms of a few, currently believed to be fundamental, constituents. Baryons consist of three quarks, while mesons are made of a quark and an antiquark. For example, the proton is made of two up-quarks and one down quark, $|p\rangle = |uud\rangle$, and the π^+-meson contains one up and one anti-down quark, $|\pi^+\rangle = |u\bar{d}\rangle$. However, the quark model in this naïve form is not complete, because the Pauli exclusion principle would not allow for a particle like the Δ isobar $|\Delta^{++}\rangle = |uuu\rangle$ with spin 3/2. The only way to construct a completely antisymmetric wavefunction for the Δ^{++} is to postulate an additional quantum number, which may be called "color". Quarks can then exist in three different color states; one may

choose calling them red, green and blue. Correspondingly, we can define a quark-state "vector" with three components,

$$q(x) = \begin{pmatrix} q^{\text{red}}(x) \\ q^{\text{green}}(x) \\ q^{\text{blue}}(x) \end{pmatrix}. \tag{1}$$

The transition from quark model to QCD is made when one decides to treat color similarly to the electric charge in electrodynamics. As is well known, the entire structure of electrodynamics emerges from the requirement of local gauge invariance, *i.e.* invariance with respect to the phase rotation of electron field, $\exp(i\alpha(x))$, where the phase α depends on the space-time coordinate. One can demand similar invariance for the quark fields, keeping in mind that while there is only one electric charge in QED, there are three color charges in QCD.

To implement this program, let us require the free quark Lagrangian,

$$\mathcal{L}_{\text{free}} = \sum_{q=u,d,s\ldots} \sum_{\text{colors}} \bar{q}(x) \left(\mathrm{i}\gamma_\mu \frac{\partial}{\partial x_\mu} - m_q \right) q(x)\,, \tag{2}$$

to be invariant under rotations of the quark fields in color space,

$$U: \qquad q^j(x) \quad \rightarrow \quad U_{jk}(x) q^k(x)\,, \tag{3}$$

with $j,k \in \{1\ldots 3\}$ (we always sum over repeated indices). Since the theory we build in this way is invariant with respect to these "gauge" transformations, all physically meaningful quantities must be gauge invariant.

In electrodynamics, there is only one electric charge, and gauge transformation involves a single phase factor, $U = \exp(i\alpha(x))$. In QCD, we have three different colors, and U becomes a (complex valued) unitary 3×3 matrix, *i.e.* $U^\dagger U = UU^\dagger = 1$, with determinant Det $U = 1$. These matrices form the fundamental representation of the group SU(3) where 3 is the number of colors, $N_{\text{c}} = 3$. The matrix U has $N_{\text{c}}^2 - 1 = 8$ independent elements and can therefore be parameterized in terms of the 8 generators T^a_{kj}, $a \in \{1\ldots 8\}$ of the fundamental representation of SU(3),

$$U(x) = \exp\left(-\mathrm{i}\phi_a(x) T^a\right)\,. \tag{4}$$

By considering a transformation U that is infinitesimally close to the **1** element of the group, it is easy to see that the matrices T^a must be Hermitian ($T^a = T^{a\dagger}$) and traceless (tr $T^a = 0$). The T^a's do not commute; instead one defines the SU(3) structure constants f_{abc} by the commutator

$$\left[T^a, T^b\right] = \mathrm{i} f_{abc} T^c. \tag{5}$$

These commutator terms have no analog in QED which is based on the abelian gauge group U(1). QCD is based on a non-abelian gauge group SU(3) and is thus called a non-abelian gauge theory.

The generators T^a are normalized to

$$\mathrm{tr}\, T^a T^b = \tfrac{1}{2}\,\delta_{ab}\,, \tag{6}$$

where δ_{ab} is the Kronecker symbol. Useful information about the algebra of color matrices, and their explicit representations, can be found in many textbooks (see, *e.g.*, [5]).

Since U is x-dependent, the free quark Lagrangian (2) is not invariant under the transformation (3). In order to preserve gauge invariance, one has to introduce, following the familiar case of electrodynamics, the gauge (or "gluon") field $A^\mu_{kj}(x)$ and replace the derivative in (2) with the so-called *covariant derivative*,

$$\partial^\mu q^j(x) \quad \to \quad D^\mu_{kj} q^j(x) \equiv \left\{ \delta_{kj}\partial^\mu - \mathrm{i} A^\mu_{kj}(x) \right\} q^j(x)\,. \tag{7}$$

Note that the gauge field $A^\mu_{kj}(x) = A^\mu_a T^a_{kj}(x)$ as well as the covariant derivative are 3×3 matrices in color space. Note also that Eq. (7) differs from the definition often given in textbooks, because we have absorbed the strong coupling constant in the field A^μ. With the replacement given by Eq. (7), all changes to the Lagrangian under gauge transformations cancel, provided A^μ transforms as

$$U: \qquad A^\mu(x) \to U(x) A^\mu(x) U^\dagger(x) + \mathrm{i} U(x) \partial^\mu U^\dagger(x)\,. \tag{8}$$

(From now on, we will often not write the color indices explicitly.)

The QCD Lagrangian then reads

$$\mathcal{L}_{\mathrm{QCD}} = \sum_q \bar{q}(x)\left(\mathrm{i}\gamma_\mu D^\mu - m_q\right) q(x) - \frac{1}{4g^2}\mathrm{tr}\; G^{\mu\nu}(x) G_{\mu\nu}(x)\,, \tag{9}$$

where the first term describes the dynamics of quarks and their couplings to gluons, while the second term describes the dynamics of the gluon field. The strong coupling constant g is the QCD analog of the elementary electric charge e in QED. The gluon field strength tensor is given by

$$G^{\mu\nu}(x) \equiv \mathrm{i}\,[D^\mu, D^\nu] = \partial^\mu A^\nu(x) - \partial^\nu A^\mu(x) - \mathrm{i}\,[A^\mu(x), A^\nu(x)]\,. \tag{10}$$

This can also be written in terms of the color components A^μ_a of the gauge field,

$$G^{\mu\nu}_a(x) = \partial^\mu A^\nu_a(x) - \partial^\nu A^\mu_a(x) + f_{abc} A^\mu_b(x) A^\nu_c(x)\,. \tag{11}$$

For a more complete presentation, see modern textbooks [5–7].

The crucial, as will become clear soon, difference between electrodynamics and QCD is the presence of the commutator on the r.h.s. of Eq. (10). This commutator gives rise to the gluon–gluon interactions that make the QCD field equations non-linear: the color fields do not simply add like in electrodynamics. These non-linearities give rise to rich and non-trivial dynamics of strong interactions.

2.2. Asymptotic freedom

Let us now turn to the discussion of the dynamical properties of QCD. To understand the dynamics of a field theory, one necessarily has to understand how the coupling constant behaves as a function of distance. This behavior, in turn, is determined by the response of the vacuum to the presence of external charge. The vacuum is the ground state of the theory; however, quantum mechanics tells us that the "vacuum" is far from being empty — the uncertainty principle allows particle–antiparticle pairs to be present in the vacuum for a period time inversely proportional to their energy. In QED, the electron–positron pairs have the effect of screening the electric charge. Thus, the electromagnetic coupling constant increases toward shorter distances. The dependence of the charge on distance is given by

$$e^2(r) = \frac{e^2(r_0)}{1 + \frac{2e^2(r_0)}{3\pi} \ln \frac{r}{r_0}}\,, \tag{12}$$

which can be obtained by resumming (logarithmically divergent, and regularized at the distance r_0) electron–positron loops dressing the virtual photon propagator.

The formula (12) has two surprising properties: first, at large distances r away from the charge which is localized at r_0, $r \gg r_0$, where one can neglect unity in the denominator, the "dressed" charge $e(r)$ becomes independent of the value of the "bare" charge $e(r_0)$ — it does not matter what the value of the charge at short distances is. Second, in the local limit $r_0 \to 0$, if we require the bare charge $e(r_0)$ be finite, the effective charge vanishes at any finite distance away from the bare charge! This is the celebrated Landau's zero charge problem [8]: the screening of the charge in QED does not allow to reconcile the presence of interactions with the local limit of the theory. This is a fundamental problem of QED, which shows that *(i)* either it is not a truly fundamental theory, or *(ii)* Eq. (12), based on perturbation theory, in the strong coupling regime gets replaced by some other expression with a more acceptable behavior. The latter possibility is quite likely since at short distances the electric charge becomes very large and its interactions with electron–positron vacuum cannot be treated perturbatively. A solution

of the zero charge problem, based on considering the rearrangement of the vacuum in the presence of "super-critical", at short distances, charge was suggested by Gribov [9].

Fortunately, because of the smallness of the physical coupling $\alpha_{\rm em}(r) = e^2(r)/(4\pi) = 1/137$, this fundamental problem of the theory manifests itself only at very short distances $\sim \exp(-3/[8\alpha_{\rm em}])$. Such short distances will probably always remain beyond the reach of experiment, and one can safely apply QED as a truly effective theory.

In QCD, as we are now going to discuss, the situation is qualitatively different, and corresponds to *anti*-screening — the charge is small at short distances and grows at larger distances. This property of the theory, discovered by Gross, Wilczek, and Politzer [11], is called asymptotic freedom.

While the derivation of the running coupling is conventionally performed by using field theoretical perturbation theory, it is instructive to see how these results can be illustrated by using the methods of condensed matter physics. Indeed, let us consider the vacuum as a continuous medium with a dielectric constant ϵ. The dielectric constant is linked to the magnetic permeability μ and the speed of light c by the relation

$$\epsilon\,\mu = \frac{1}{c^2} = 1\,. \tag{13}$$

Thus, a screening medium ($\epsilon > 1$) will be diamagnetic ($\mu < 1$), and conversely a paramagnetic medium ($\mu > 1$) will exhibit anti-screening which leads to asymptotic freedom. In order to calculate the running coupling constant, one has to calculate the magnetic permeability of the vacuum. We follow [12] in our discussion, where this has been done in a framework very similar to Landau's theory of the diamagnetic properties of a free electron gas. In QED one has

$$\epsilon_{\rm QED} = 1 + \frac{2e^2(r_0)}{3\pi}\ln\frac{r}{r_0} > 1\,. \tag{14}$$

So why is the QCD vacuum paramagnetic while the QED vacuum is diamagnetic? The energy density of a medium in the presence of an external magnetic field $\vec{B}$ is given by

$$u = -\frac{1}{2}4\pi\chi\vec{B}^2\,, \tag{15}$$

where the magnetic susceptibility χ is defined by the relation

$$\mu = 1 + 4\pi\chi\,. \tag{16}$$

When electrons move in an external magnetic field, two competing effects determine the sign of magnetic susceptibility:

- The electrons in magnetic field move along quantized orbits, so-called Landau levels. The current originating from this movement produces a magnetic field with opposite direction to the external field. This is the diamagnetic response, $\chi < 0$.

- The electron spins align along the direction of the external $\vec{B}$-field, leading to a paramagnetic response ($\chi > 0$).

In QED, the diamagnetic effect is stronger, so the vacuum is screening the bare charges. In QCD, however, gluons carry color charge. Since they have a larger spin (spin 1) than quarks (or electrons), the paramagnetic effect dominates and the vacuum is anti-screening.

Let us explain this in more detail. Basing on the considerations given above, the energy density of the QCD vacuum in the presence of an external color-magnetic field can be calculated by using the standard formulas of quantum mechanics, see *e.g.* [13], by summing over Landau levels and taking account of the fact that gluons and quarks give contributions of different sign. Note that a summation over all Landau levels would lead to an infinite result for the energy density. In order to avoid this divergence, one has to introduce a cutoff Λ with dimension of mass. Only field modes with wavelength $\lambda \gtrsim 1/\Lambda$ are taken into account. The upper limit for λ is given by the radius of the largest Landau orbit, $r_0 \sim 1/\sqrt{gB}$, which is the only dimensionful scale in the problem; the summation thus is made over the wave lengths satisfying

$$\frac{1}{\sqrt{|gB|}} \gtrsim \lambda \gtrsim \frac{1}{\Lambda}\,, \tag{17}$$

The result is [12]

$$u_{\rm vac}^{\rm QCD} = -\frac{1}{2}B^2\frac{11N_{\rm c}-2N_{\rm f}}{48\pi^2}g^2\ln\frac{\Lambda^2}{|gB|}\,, \tag{18}$$

where $N_{\rm f}$ is the number of quark flavors, and $N_{\rm c}=3$ is the number of flavors. Comparing this with Eqs. (15) and (16), one can read off the magnetic permeability of the QCD vacuum,

$$\mu_{\rm vac}^{\rm QCD}(B) = 1 + \frac{11N_{\rm c}-2N_{\rm f}}{48\pi^2}g^2\ln\frac{\Lambda^2}{|gB|} > 1\,. \tag{19}$$

The first term in the denominator ($11N_{\rm c}$) is the gluon contribution to the magnetic permeability. This term dominates over the quark contribution ($2N_{\rm f}$) as long as the number of flavors $N_{\rm f}$ is less than 17 and is responsible for asymptotic freedom.

The dielectric constant as a function of distance r is then given by

$$\epsilon_{\rm vac}^{\rm QCD}(r) = \left.\frac{1}{\mu_{\rm vac}^{\rm QCD}(B)}\right|_{\sqrt{|gB|}\to 1/r} . \tag{20}$$

The replacement $\sqrt{|gB|} \to 1/r$ follows from the fact that ϵ and μ in Eq. (20) should be calculated from the same field modes: the dielectric constant $\epsilon(r)$ could be calculated by computing the vacuum energy in the presence of two static colored test particles located at a distance r from each other. In this case, the maximum wavelength of field modes that can contribute is of order r so that

$$r \gtrsim \lambda \gtrsim \frac{1}{\Lambda} . \tag{21}$$

Combining Eqs. (17) and (21), we identify $r = 1/\sqrt{|gB|}$ and find

$$\epsilon_{\rm vac}^{\rm QCD}(r) = \frac{1}{1 + \frac{11N_{\rm c}-2N_{\rm f}}{24\pi^2} g^2 \ln(r\Lambda)} < 1 . \tag{22}$$

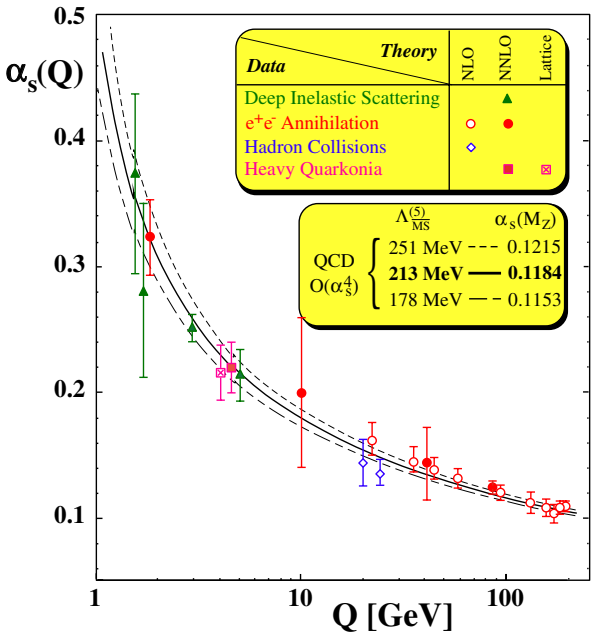

Fig. 1. The running coupling constant $\alpha_{\rm s}(Q^2)$ as a function of momentum transfer Q^2 determined from a variety of processes. The figure is from [14], courtesy of S. Bethke.

With $\alpha_{\rm s}(r_1)/\alpha_{\rm s}(r_2) = \epsilon_{\rm vac}^{\rm QCD}(r_2)/\epsilon_{\rm vac}^{\rm QCD}(r_1)$ one finds to lowest order in $\alpha_{\rm s}$

$$\alpha_{\rm s}(r_1) = \frac{\alpha_{\rm s}(r_2)}{1 + \frac{11N_{\rm c}-2N_{\rm f}}{6\pi}\alpha_{\rm s}(r_2)\ln\left(\frac{r_2}{r_1}\right)}. \tag{23}$$

Apparently, if $r_1 < r_2$ then $\alpha_{\rm s}(r_1) < \alpha_{\rm s}(r_2)$. The running of the coupling constant is shown in Fig. 1, $Q \sim 1/r$. The intuitive derivation given above illustrates the original field-theoretical result of [11].

At high momentum transfer, corresponding to short distances, the coupling constant thus becomes small and one can apply perturbation theory, see Fig. 1. There is a variety of processes that involve high momentum scales, *e.g.* deep inelastic scattering, Drell–Yan dilepton production, e^+e^--annihilation into hadrons, production of heavy quarks/quarkonia, high $p_{\rm T}$ hadron production .... QCD correctly predicts the Q^2 dependence of these, so-called "hard" processes, which is a great success of the theory.

2.3. Confinement

While asymptotic freedom implies that the theory becomes simple and treatable at short distances, it also tells us that at large distances the coupling becomes very strong. In this regime we have no reason to believe in perturbation theory. In QED, as we have discussed above, the strong coupling regime starts at extremely short distances beyond the reach of current experiments — and this makes the "zero-charge" problem somewhat academic. In QCD, the entire physical World around us is defined by the properties of the theory in the strong coupling regime — and we have to construct accelerators to study it in the much more simple, "QED-like", weak coupling limit.

We do not have to look far to find the striking differences between the properties of QCD at short and large distances: the elementary building blocks of QCD — the "fundamental" fields appearing in the Lagrangian (9), quarks and gluons, do not exist in the physical spectrum as asymptotic states. For some, still unknown to us, reason, all physical states with finite energy appear to be color-singlet combinations of quarks and gluons, which are thus always "confined" at rather short distances on the order of 1 fm. This prevents us, at least in principle, from using well-developed formal S-matrix approaches based on analyticity and unitarity to describe quark and gluon interactions.

The property of confinement can be explored by looking at the propagation of heavy quark–antiquark pair at a distance R propagating in time a distance T. An object which describes the behavior of this system is the

Wilson loop [15]

$$W(R,T) = \mathrm{Tr}\left[P \exp\left[i \int\limits_C A_\mu^a T^a dx^\mu\right]\right], \tag{24}$$

where A_μ^a is the gluon field, T^a is the generator of SU(3), and the contour C is chosen as a rectangle with side R in one of the space dimensions and T in the time direction. It can be shown that at large T the asymptotics of the Wilson loop is

$$\lim_{T\to\infty} W(R,T) = \exp\left[-TV(R)\right], \tag{25}$$

where $V(R)$ is the static potential acting between the heavy quarks. At large distances, this potential grows as

$$V(R) = \sigma R, \tag{26}$$

where $\sigma \sim 1$ GeV/fm is the string tension. We thus conclude that at large T and R the Wilson loop should behave as

$$W(R,T) \simeq \exp\left[-\sigma TR\right], \tag{27}$$

The formula (27) is the celebrated "area law", which signals confinement.

It should be noted, however, that the introduction of dynamical quarks leads to the string break-up at large distances, and the potential $V(R)$ saturates at a constant. The presence of light dynamical quarks is most important in Gribov's confinement scenario [9], in which the color charges at large distances behave similarly to the "supercritical" charge in electrodynamics, polarizing the vacuum and producing copious quark–antiquark pairs which screen them. In this scenario, in the physical world with light quarks there is never a confining force acting on color charges at large distances, just quark–antiquark pair production ("soft confinement"); for a review of the approach and recent developments, see [10]. This may explain why the spectra of jets, for example, computed in perturbative QCD, appear to be consistent with experiment; this fact would be difficult to reconcile with the existence of strong confining forces. There exists a special situation, however, when the law (27) should be appropriate even in the presence of light quarks — the heavy quarkonium. The sizes of heavy quarkonia are quite small, and their masses are below the threshold to produce a pair of heavy mesons. This is why heavy quarkonia are especially useful probes of confinement.

At high temperatures, the long-range interactions responsible for confinement become screened away — instead of the growing potential (26), we expect

$$V(R) \sim -\frac{g^2(T)}{R} \exp(-m_{\mathrm{D}} R), \tag{28}$$

where $m_{\rm D} \sim gT$ is the Debye mass. Mathematically, this transition to the deconfined phase can again be studied by looking at the properties of the Wilson loop. At finite temperature, the theory is defined on a cylinder: Euclidean time τ varies within $0 \leq \tau \leq \beta = 1/T$, and the gluon fields satisfy the periodic boundary conditions:

$$A^a_\mu(\vec{x}, 0) = A^a_\mu(\vec{x}, \beta)\,. \tag{29}$$

Let us now consider the Wilson loop wrapped around this cylinder (the Polyakov loop), and choose a gauge where A^a_0 is time-independent:

$$P(\vec{x}) = \mathrm{Tr} \exp\left[ig\beta A^a_0(\vec{x})t^a\right]; \tag{30}$$

the correlation function of these objects can be defined as

$$C_T(\vec{x}) = \langle P(\vec{x})P^*(\vec{x})\rangle_T\ . \tag{31}$$

Again, it can be shown that this correlation function is related to the free energy, and thus static potential $V(R)$, of the heavy quark–antiquark pair. Assuming, as before, that the heavy quarks are separated by the spatial distance $R = |\vec{x}|$, one finds

$$C_T(R) \sim \exp\left[-\beta V(R)\right]. \tag{32}$$

Again, if we define the limit value $L(T)$ of the correlation function,

$$\lim_{R\to\infty}\ C_T(R) \equiv L(T) \tag{33}$$

it would have to vanish in the confined phase in the absence of dynamical quarks, since $V(R)$ tends to infinity in this case: $L(T) = 0$. In the deconfined phase, on the other hand, because of the screening $V(R)$ should tend to a constant, and this implies a finite value $L(T) \neq 0$. The correlation function of Polyakov loops therefore can be used as an order parameter of the deconfinement. The behavior of $L(T)$ as a function of temperature has been measured on the lattice; one indeed observes a transition from the confined phase with $L(T) = 0$ to the deconfined phase with $L(T) \neq 0$ at some critical temperature $T_{\rm c}$. In the presence of light quarks, as we have already discussed above, the potential would tend to a constant even in the confined phase, and $L(T)$ ceases to be a rigorous order parameter.

2.4. Chiral symmetry breaking

The decades of experience with "soft pion" techniques and current algebra convinced physicists that the properties of the world with massless pions are quite close to the properties of our physical World. The existence of massless particles is always a manifestation of a symmetry of the theory — photons, for example, appear as a consequence of local gauge invariance of the electrodynamics. However, unlike photons, pions have zero spin and cannot be gauge bosons of any symmetry. The other possibility is provided by the Goldstone theorem, which states that the appearance of massless modes in the spectrum can also reflect a spontaneously broken symmetry, *i.e.* the symmetry of the theory which is broken in the ground state. Because of the great importance of this theorem, let us briefly sketch its proof.

Suppose that the Hamiltonian H of the theory is invariant under some symmetry generated by operators Q_i, so that

$$[H, Q_i] = 0\,. \tag{34}$$

Spontaneous symmetry breaking in the ground state of theory implies that for some of the generators Q_i

$$Q_i|0\rangle \neq 0\,. \tag{35}$$

Since Q_i commute with the Hamiltonian, this means that this new state $Q_i|0\rangle$ has the same energy as the ground state. The vacuum is therefore degenerate, and in a relativistically invariant theory this implies the existence of massless particles — Goldstone bosons. A useful example of that is provided by the phonons in a crystal, where the continuous translational symmetry of the QED Lagrangian is spontaneously broken by the existence of the fixed period of the crystal lattice.

Even though all six quark flavors enter the Lagrangian, it is intuitively clear that at small scales $Q \ll M_c, M_b, M_t$, heavy quarks should not have any influence on the dynamics. In a rigorous way this statement is formulated in terms of decoupling theorems, which we will discuss in detail later. At the moment let us just assume that we are interested in the low-energy behavior, and that only light quarks are relevant for that purpose. Then it makes sense to consider the approximate symmetry, which becomes exact when the quarks are massless. In fact, in this limit, the Lagrangian does not contain any terms which connect the right- and left-handed components of the quark fields:

$$q_{\rm R} = \tfrac{1}{2}(1+\gamma_5)q\,, \qquad q_{\rm L} = \tfrac{1}{2}(1-\gamma_5)q\,. \tag{36}$$

The Lagrangian of QCD (9) is therefore invariant under the independent transformations of right- and left-handed fields ("chiral rotations"). In the

limit of massless quarks, QCD thus possesses an additional symmetry $U_{\rm L}(N_{\rm f}) \times U_{\rm R}(N_{\rm f})$ with respect to the independent transformation of left- and right-handed quark fields $q_{\rm L,R} = \frac{1}{2}(1 \pm \gamma_5)q$:

$$q_{\rm L} \to V_{\rm L} q_{\rm L}\,, \quad q_{\rm R} \to V_{\rm R} q_{\rm R}\,, \quad V_{\rm L}, V_{\rm R} \in U(N_{\rm f})\,, \tag{37}$$

this means that left- and right-handed quarks are not correlated.

Even a brief look into the Particle Data tables, or simply in the mirror, can convince anyone that there is no symmetry between left and right in the physical World. One thus has to assume that the symmetry (37) is spontaneously broken in the vacuum.

The presence of the "quark condensate" $\langle\bar{q}q\rangle$ in QCD vacuum signals spontaneous breakdown of this symmetry, since

$$\langle\bar{q}q\rangle = \langle\bar{q_{\rm L}} q_{\rm R}\rangle + \langle\bar{q_{\rm R}} q_{\rm L}\rangle\,, \tag{38}$$

which means that left- and right-handed quarks and antiquarks can transform into each other. Quark condensate therefore can be used as an order parameter of chiral symmetry. Lattice calculations show that around the deconfinement phase transition, quark condensate dramatically decreases, signaling the onset of the chiral symmetry restoration.

This spontaneous breaking of $\mathrm{U_L}(3)\times\mathrm{U_R}(3)$ chiral symmetry, by virtue of the Goldstone theorem presented above, should give rise to $3^2 = 9$ Goldstone particles. The flavor composition of the existing eight candidates for this role (3 pions, 4 kaons, and the η) suggests that the $\mathrm{U_A}(1)$ part of $\mathrm{U_L}(3)\times\mathrm{U_R}(3) = \mathrm{SU_L}(3)\times\mathrm{SU_R}(3)\times\mathrm{U_V}(1)\times\mathrm{U_A}(1)$ does not exist. This constitutes the famous "$\mathrm{U_A}(1)$ problem".

There is yet another problem with the chiral limit in QCD. Indeed, as the quark masses are put to zero, the Lagrangian (9) does not contain a single dimensionful scale — the only parameters are pure numbers $N_{\rm c}$ and $N_{\rm f}$. The theory is thus apparently invariant with respect to scale transformations, and the corresponding scale current is conserved: $\partial_\mu s_\mu = 0$. However, the absence of a mass scale would imply that all physical states in the theory should be massless!

2.5. Quantum anomalies

Both apparent problems — the missing $\mathrm{U_A}(1)$ symmetry and the origin of hadron masses — are related to quantum anomalies. A symmetry of a classical theory can be broken when that theory is quantized, due to the requirements of regularization and renormalization. This is called anomalous symmetry breaking. Regularization of the theory on the quantum level brings in a dimensionful parameter — remember the cutoff Λ of Eq. (17) we had to impose on the wavelength of quarks and gluons.

Once the theory is quantized, we already know that the coupling constant is scale dependent and therefore scale invariance is broken (note that the four-divergence of the scale current in field theory is equal to the trace of the energy momentum tensor Θ^μ_μ). One finds

$$\partial^\mu s_\mu = \Theta^\mu_\mu = \sum_q m_q \bar{q} q + \frac{\beta(g)}{2g^3} \mathrm{tr} \mathrm{G}^{\mu\nu} \mathrm{G}_{\mu\nu}, \tag{39}$$

where $\beta(g)$ is the QCD β-function, which governs the behavior of the running coupling:

$$\mu \frac{dg(\mu)}{d\mu} = \beta(g)\,, \tag{40}$$

note that as discussed in Section 2.1 we include coupling g in the definition of the gluon fields. As we already discussed, at small coupling g, the β function is negative, which means that the theory is asymptotically free. The leading term in the perturbative expansion is (compare with Eq. (23))

$$\beta(g) = -b \frac{g^3}{(4\pi)^2} + O(g^5), \qquad b = 11 N_\mathrm{c} - 2 N_\mathrm{f}, \tag{41}$$

where N_c and N_f are the numbers of colors and flavors, respectively.

Hadron masses are related to the forward matrix element of trace of the QCD energy-momentum tensor, $2m_\mathrm{h}^2 = \langle h | \Theta^\mu_\mu | h \rangle$. Apparently, light hadron masses must receive dominant contributions from the G^2-term in Eq. (39). Note also that the flavor sum in Eq. (39) includes heavy flavors, too. This would lead to the unphysical picture that *e.g.* the proton mass is dominated by heavy quark masses. However, the heavy flavor contribution to the sum (39) is exactly canceled by a corresponding heavy flavor contribution to the β-function.

2.6. The strong CP problem and "θ-worlds"

Similar anomaly appears in the divergence of the axial current, $j^5_\mu = \bar{q} \gamma_\mu \gamma^5 q$, generated by the $\mathrm{U_A}(1)$ group. The corresponding axial charge is not conserved because of the contribution of the triangle graph and the four-divergence of the axial current is given by [16]

$$\partial^\mu j^5_\mu = \sum_q 2\mathrm{i} m_q \bar{q} \gamma^5 q + \frac{N_\mathrm{f}}{8\pi^2} \mathrm{Tr}\, G^{\mu\nu} \widetilde{G}_{\mu\nu}\,, \tag{42}$$

where $\widetilde{G}_{\mu\nu} = \epsilon_{\mu\nu\kappa\lambda} G^{\kappa\lambda}/2$ is the dual field strength tensor. Since the gluonic part on the r.h.s. of this equation is a surface term (a full divergence), there would be no physical effect, if the QCD vacuum were "empty".

However, it appears that due to non-trivial topology of the SU(3) gauge group, QCD equations of motion allow classical solutions even in the absence of external color source, *i.e.* in the vacuum. The well-known example of a classical solution is the *instanton*, corresponding to the mapping of a three-dimensional sphere S^3 onto the SU(2) subgroup of color SU(3) (for reviews, see [17,18]). As a result, the ground state of classical Chromodynamics is not unique. There is an enumerable infinite number of gauge field configurations with different topologies (corresponding to different winding number in the $S^3 \to \mathrm{SU}(2)$ mapping), and the ground state looks like a periodic potential.

In a quantum theory, however, the system will not stay in one of the minima, like the classical system would. Instead, there will be tunneling processes between different minima. These tunneling processes, in Minkowski space, correspond to instantons. Since tunneling, in general, lowers the ground state energy of the system, one expects the QCD vacuum to have a complicated structure.

Instantons, through the anomaly relation (42), lead to the explicit violation of the $\mathrm{U}_A(1)$ symmetry and thus solve the mystery of the missing ninth Goldstone boson — the η'. Physically, axial symmetry $\mathrm{U}_A(1)$ is broken because the tunneling processes between topologically different vacua are accompanied by the change in quark helicity — even in the vacuum, left-handed quarks periodically turn into right-handed and *vice versa*.

The periodic vacuum structure immediately leads to a puzzle known as the *strong CP problem:* When one calculates the expectation value of an observable in the vacuum, one has to average over all topological sectors of the vacuum. This is equivalent to adding an additional term to the QCD-Lagrangian,

$$\mathcal{L}_{\mathrm{QCD}} \to \mathcal{L}_{\mathrm{QCD}} - \frac{\theta}{16\pi^2}\ \mathrm{Tr}\ G^{\mu\nu}\widetilde{G}_{\mu\nu}\,, \tag{43}$$

where $\theta \in [0, 2\pi]$ is a parameter of the theory which has to be determined from experiment. Since the θ-term in Eq. (43) is CP violating, a non-zero value of θ would have immediate phenomenological consequences, *e.g.* an electric dipole moment of the neutron. However, precision measurements of this dipole moment constrain θ to $\theta < 10^{-9}$. The fact that θ is so unnaturally small constitutes the strong CP problem. The most likely solution to this problem [19] implies the existence of a light pseudoscalar meson, the *axion*. However, despite many efforts, axions remain unobserved in experiment.

2.7. The phase structure of QCD

As was repeatedly stated above, the most important problem facing us in the study of all aspects of QCD is understanding the structure of the vacuum, which, in a manner of saying, does not at all behave as an empty

space, but as a physical entity with a complicated structure. As such, the vacuum can be excited, altered and modified in physical processes [20]. For a comprehensive review of the phase structure of QCD, see [21].

Collisions of heavy ions are the best way to create high energy density in a "macroscopic" (on the scale of a single hadron) volume. It thus could be possible to create and to study a new state of matter, the *Quark–Gluon Plasma* (QGP), in which quarks and gluons are no longer confined in hadrons, but can propagate freely. The search for QGP is one of the main motivations for the heavy ion research.

Lattice calculations predict that QCD at high temperatures undergoes phase transitions in which confinement property is lost and chiral symmetry is restored. The critical temperature for the chiral phase transition is about equal to the critical temperature for deconfinement; for a recent overview, see [22].

Heavy ion collisions at RHIC may also give us the possibility to study the θ angle dependence of the QCD phase diagram. In a heavy ion collision, bubbles containing a metastable vacuum with $\theta \neq 0$ may be produced, and may reveal themselves through their unusual decay pattern [23]; the first preliminary experimental results regarding the charge asymmetry of the produced pions with respect to reaction plane have become available [24].

3. The strong field limit of QCD

3.1. QCD in the classical regime

Most of the applications of QCD so far have been limited to the short distance regime of high momentum transfer, where the theory becomes weakly coupled. While this is the only domain where our theoretical tools based on perturbation theory are adequate, this is also the domain in which the beautiful non-linear structure of QCD does not yet reveal itself fully. On the other hand, as soon as we decrease the momentum transfer in a process, the dynamics rapidly becomes non-linear, but our understanding is hindered by the large coupling. Being perplexed by this problem, one is tempted to dream about an environment in which the coupling is weak, allowing a systematic theoretical treatment, but the fields are strong, revealing the full non-linear nature of QCD. We are going to argue now that this environment is realized in high energy collisions. Hadron and especially heavy ion collisions at very high energies allow to probe QCD in the non-linear regime of high parton density and high color field strength, see Fig. 2.

It has been conjectured long time ago that the dynamics of QCD in the high density domain may become qualitatively different: in parton language, this is best described in terms of *parton saturation* [26–28], and in the language of color fields — in terms of the *classical* Chromo-Dynamics [29]; see

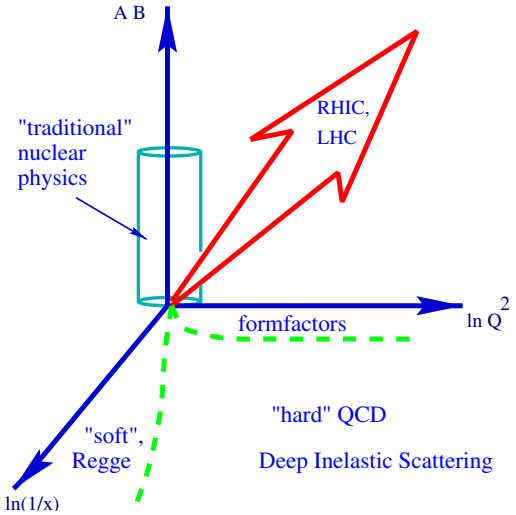

Fig. 2. The place of relativistic heavy ion physics in the study of QCD; the vertical axis is the product of atomic numbers of projectile and target, and the horizontal axes are the momentum transfer Q^2 and rapidity $y = \ln(1/x)$ (x is the Bjorken scaling variable).

the lectures [30] and [31] and references therein. In this high density regime, the transition amplitudes are dominated not by quantum fluctuations, but by the configurations of classical field containing large, $\sim 1/\alpha_{\rm s}$, numbers of gluons. One thus uncovers new non–linear features of QCD, which cannot be investigated in the more traditional applications based on the perturbative approach. The classical color fields in the initial nuclei (the "color glass condensate" [30]) can be thought of as either perturbatively generated, or as being a topologically non-trivial superposition of the Weizsäcker–Williams radiation and the quasi-classical vacuum fields [32–34].

3.2. Geometrical arguments

Let us consider an external probe J interacting with the nuclear target of atomic number A. At small values of Bjorken x, by uncertainty principle the interaction develops over large longitudinal distances $z \sim 1/mx$, where m is the nucleon mass. As soon as z becomes larger than the nuclear diameter, the probe cannot distinguish between the nucleons located on the front and back edges of the nucleus, and all partons within the transverse area $\sim 1/Q^2$ determined by the momentum transfer Q participate in the interaction coherently. The density of partons in the transverse plane is given by

$$\rho_A \simeq \frac{xG_A(x,Q^2)}{\pi R_A^2} \sim A^{1/3}, \tag{44}$$

where we have assumed that the nuclear gluon distribution scales with the number of nucleons A. The probe interacts with partons with cross section $\sigma \sim \alpha_{\rm s}/Q^2$; therefore, depending on the magnitude of momentum transfer Q, atomic number A, and the value of Bjorken x, one may encounter two regimes:

- $\sigma\rho_A \ll 1$ — this is a familiar "dilute" regime of incoherent interactions, which is well described by the methods of perturbative QCD;

- $\sigma\rho_A \gg 1$ — in this regime, we deal with a dense parton system. Not only do the "leading twist" expressions become inadequate, but also the expansion in higher twists, *i.e.* in multi-parton correlations, breaks down here.

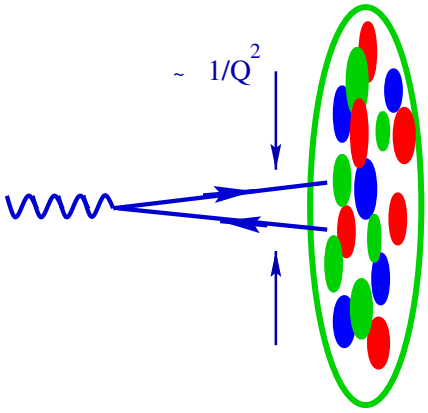

Fig. 3. Hard probe interacting with the nuclear target resolves the transverse distance $\sim 1/\sqrt{Q}$ (Q^2 is the square of the momentum transfer) and, in the target rest frame, the longitudinal distance $\sim 1/(mx)$ (m is the nucleon mass and x the Bjorken variable).

The border between the two regimes can be found from the condition $\sigma\rho_A \simeq 1$; it determines the critical value of the momentum transfer ("saturation scale" [26]) at which the parton system becomes to look dense to the probe[1]:

$$Q_{\rm s}^2 \sim \alpha_{\rm s}\,\frac{xG_A(x,Q_{\rm s}^2)}{\pi R_A^2}\,. \tag{45}$$

[1] Note that since $Q_{\rm s}^2 \sim A^{1/3}$, which is the length of the target, this expression in the target rest frame can also be understood as describing a broadening of the transverse momentum resulting from the multiple re-scattering of the probe.

In this regime, the number of gluons from (45) is given by

$$xG_A(x,Q_{\rm s}^2) \sim \frac{\pi}{\alpha_{\rm s}(Q_{\rm s}^2)}\ Q_{\rm s}^2 R_A^2\,, \tag{46}$$

where $Q_{\rm s}^2 R_A^2 \sim A$. One can see that the number of gluons is proportional to the *inverse* of $\alpha_{\rm s}(Q_{\rm s}^2)$, and becomes large in the weak coupling regime. In this regime, as we shall now discuss, the dynamics is likely to become essentially classical.

3.3. Saturation as the classical limit of QCD

Indeed, the condition (45) can be derived in the following, rather general, way. As a first step, let us note that the dependence of the action corresponding to the Lagrangian (9) on the coupling constant is given by

$$S \sim \int \frac{1}{g^2}\ G^a_{\mu\nu} G^a_{\mu\nu}\ d^4x\,. \tag{47}$$

Let us now consider a classical configuration of gluon fields; by definition, $G^a_{\mu\nu}$ in such a configuration does not depend on the coupling, and the action is large, $S \gg \hbar$. The number of quanta in such a configuration is then

$$N_g \sim \frac{S}{\hbar} \sim \frac{1}{\hbar\ g^2}\ \rho_4 V_4\,, \tag{48}$$

where we re-wrote (47) as a product of four-dimensional action density ρ_4 and the four-dimensional volume V_4.

Note that since (48) depends only on the product of the Planck constant $\hbar$ and the coupling g^2, the classical limit $\hbar \to 0$ is indistinguishable from the weak coupling limit $g^2 \to 0$. The weak coupling limit of small $g^2 = 4\pi\alpha_{\rm s}$ therefore corresponds to the semi-classical regime.

The effects of non-linear interactions among the gluons become important when $\partial_\mu A_\mu \sim A_\mu^2$ (this condition can be made explicitly gauge invariant if we derive it from the expansion of a correlation function of gauge-invariant gluon operators, *e.g.*, G^2). In momentum space, this equality corresponds to

$$Q_{\rm s}^2 \sim (A_\mu)^2 \sim (G^2)^{1/2} = \sqrt{\rho_4}\,. \tag{49}$$

$Q_{\rm s}$ is the typical value of the gluon momentum below which the interactions become essentially non-linear.

Consider now a nucleus A boosted to a high momentum. By uncertainty principle, the gluons with transverse momentum $Q_{\rm s}$ are extended in the longitudinal and proper time directions by $\sim 1/Q_{\rm s}$; since the transverse

area is πR_A^2, the four-volume is $V_4 \sim \pi R_A^2/Q_s^2$. The resulting four-density from (48) is then

$$\rho_4 \sim \alpha_s \, \frac{N_g}{V_4} \sim \alpha_s \, \frac{N_g \, Q_s^2}{\pi R_A^2} \sim Q_s^4 \,, \tag{50}$$

where at the last stage we have used the non-linearity condition (49), $\rho_4 \sim Q_s^4$. It is easy to see that (50) coincides with the saturation condition (45), since the number of gluons in the infinite momentum frame $N_g \sim xG(x, Q_s^2)$.

In view of the significance of saturation criterion for the rest of the material in these lectures, let us present yet another argument, traditionally followed in the discussion of classical limit in electrodynamics [35]. The energy of the gluon field per unit volume is $\sim \vec{E}^{a2}$. The number of elementary "oscillators of the field", also per unit volume, is $\sim \omega^3$. To get the number of the quanta in the field we have to divide the energy of the field by the product of the number of the oscillators $\sim \omega^3$ and the average energy $\hbar\omega$ of the gluon:

$$N_{\vec{k}} \sim \frac{\vec{E}^{a2}}{\hbar\omega^4} \,. \tag{51}$$

The classical approximation holds when $N_{\vec{k}} \gg 1$. Since the energy ω of the oscillators is related to the time Δt over which the average energy is computed by $\omega \sim 1/\Delta t$, we get

$$\vec{E}^{a2} \gg \frac{\hbar}{(\Delta t)^4} \,. \tag{52}$$

Note that the quantum mechanical uncertainty principle for the energy of the field reads

$$\vec{E}^{a2} \; \omega^4 \sim \hbar \,, \tag{53}$$

so the condition (52) indeed defines the quasi-classical limit.

Since $\vec{E}^{a2}$ is proportional to the action density ρ_4, and the typical time is $\Delta t \sim 1/k_\perp$, using (50) we finally get that the classical description applies when

$$k_\perp^2 < \alpha_s \frac{N_g}{\pi R_A^2} \equiv Q_s^2 \,. \tag{54}$$

3.4. Saturation and gluon correlations

When the occupation numbers of the field become large, the matrix elements of the creation and annihilation operators of the gluon field defined by

$$\hat{A}^\mu = \sum_{\vec{k},\alpha} \left(\hat{c}_{\vec{k}\alpha} A^\mu_{\vec{k}\alpha} + \hat{c}^\dagger_{\vec{k}\alpha} A^{\mu *}_{\vec{k}\alpha} \right) \tag{55}$$

become very large,

$$N_{\vec{k}\alpha} = \langle \hat{c}^{\dagger}_{\vec{k}\alpha} \hat{c}_{\vec{k}\alpha} \rangle \gg 1 \,, \tag{56}$$

so that one can neglect the unity on the r.h.s. of the commutation relation

$$\hat{c}_{\vec{k}\alpha} \hat{c}^{\dagger}_{\vec{k}\alpha} - \hat{c}^{\dagger}_{\vec{k}\alpha} \hat{c}_{\vec{k}\alpha} = 1 \tag{57}$$

and treat these operators as classical c-numbers.

This observation, often used in condensed matter physics, especially in the theoretical treatment of superfluidity, has important consequences for gluon production — in particular, it implies that the correlations among the gluons in the saturation region can be neglected:

$$\langle A(k_1) A(k_2) \dots A(k_n) \rangle \simeq \langle A(k_1) \rangle \langle A(k_2) \rangle \dots \langle A(k_n) \rangle \,. \tag{58}$$

Thus, in contrast to the perturbative picture, where the produced mini-jets have strong back-to-back correlations, the gluons resulting from the decay of the classical saturated field are uncorrelated at $k_\perp \lesssim Q_{\rm s}$. The traces of this phenomenon are expected to extend even to larger transverse momenta, especially when the produced gluons are separated by a significant rapidity window [36].

Note that the amplitude with the factorization property (58) is called point-like. However, the relation (58) cannot be exact if we consider the correlations of final-state hadrons — the gluon mini-jets cannot transform into hadrons independently. These correlations caused by color confinement however affect mainly hadrons with close three-momenta, as opposed to the perturbative correlations among mini-jets with the opposite three-momenta.

It will be interesting to explore the consequences of the factorization property of the classical gluon field (58) for the HBT correlations of final–state hadrons. It is likely that the HBT radii in this case reflect the universal color correlations in the hadronization process.

Another interesting property of classical fields follows from the relation

$$\left\langle \left(\hat{c}^{\dagger}_{\vec{k}\alpha} \hat{c}_{\vec{k}\alpha} \right)^2 \right\rangle - \left\langle \hat{c}^{\dagger}_{\vec{k}\alpha} \hat{c}_{\vec{k}\alpha} \right\rangle^2 = \left\langle \hat{c}^{\dagger}_{\vec{k}\alpha} \hat{c}_{\vec{k}\alpha} \right\rangle \,, \tag{59}$$

which determines the fluctuations in the number of produced gluons. We will discuss the implications of Eq. (59) for the multiplicity fluctuations in heavy ion collisions later.

3.5. Renormalization group and the effective action

Above we gave arguments in favor of the applicability of classical approach to the description of QCD in the regime of strong color fields. However, the dynamics of strong color fields cannot be entirely classical because

of the asymptotic freedom of QCD (see Section 2.2) and the related scale anomaly discussed in section 2.5. Moreover, as we shall see, the applicability of the classical approach to the description of strong color fields hinges upon the asymptotic freedom.

The QCD renormalization group constraints can be described by an effective action of the following form [37] (see also [38–40]):

$$\mathcal{L}_{\rm eff} = -\frac{1}{4\bar{g}^2(t)}\, G^2, \quad t \equiv \ln\left(\frac{G^2}{\Lambda^4}\right), \tag{60}$$

where $G^2 \equiv \mathrm{Tr}\; G^{\mu\nu}(x) G_{\mu\nu}(x)$; since we are interested in the dynamics of gauge fields, we kept only the gluon part of Eq. (9). The coupling $\bar{g}(t)$ in Eq. (60) is defined implicitly by renormalization group through the relation

$$t = \int\limits_{g}^{\bar{g}(t)} \frac{dg}{\beta(g)}\,, \tag{61}$$

where $\beta(g)$ is the β function of QCD, Eq. (41). At large t (the limit of strong color field), Eq. (61) yields the following behavior:

$$\frac{1}{\bar{g}^2(t)} \sim t + \dots\,. \tag{62}$$

Therefore, in the regime of strong color fields the effective action behaves as

$$\mathcal{L}_{\rm eff} \sim G^2\; \ln\left(\frac{G^2}{\Lambda^4}\right), \tag{63}$$

which shows that in the limit of strong field the dynamics in QCD is controlled by small coupling $\sim \ln^{-1}(G^2/\Lambda^2)$. According to the arguments given in Section 3.3 and equations Eq. (48) and Eq. (49), this translates into the following expectation [41] for the number of gluons in a nucleus A on the saturation momentum $Q_{\rm s}$:

$$N_g \sim \pi R_A^2\; Q_{\rm s}^2\; \ln\left(\frac{Q_{\rm s}^2}{\Lambda^2}\right). \tag{64}$$

Before we proceed to the test of Eq. (64) in high energy collisions, a few more words about the implications of the effective action Eq. (60). In Minkowski space, $G^2 = 2(H^2 - E^2)$ where E and H are the chromo-electric and chromo-magnetic fields, respectively. The effective action Eq. (60) is real only if $H^2 \geq E^2$, which may serve as a hint of magnetic condensation in the ground state of QCD. For strong predominantly chromo-electric fields when

$E^2 > H^2$ the action Eq. (60) acquires an imaginary part $\mathrm{Im}\mathcal{L}_{\mathrm{eff}} \sim E^2$, which signals an instability — such a field after being created will decay by the production of pairs of gluons and quarks. The corresponding scenario for high-energy collisions has been considered in Ref. [42]; the chromo-electric fields formed in this case are predominantly longitudinal [42–44].

The renormalization properties of QCD encoded in the effective action thus imply both the logarithmic correction to the number of gluons in a classical field configuration Eq. (64) and the quantum contribution to the decay of such a configuration through pair production.

4. Classical QCD and high energy collisions

4.1. Centrality dependence of hadron production

In nuclear collisions, the saturation scale becomes a function of centrality; a generic feature of the quasi-classical approach — the proportionality of the number of gluons to the inverse of the coupling constant (48) — thus leads to definite predictions [41] on the centrality dependence of multiplicity.

Let us first present the argument on a qualitative level. At different centralities (determined by the impact parameter of the collision), the average density of partons (in the transverse plane) participating in the collision is very different. This density ρ is proportional to the average length of nuclear material involved in the collision, which in turn approximately scales with the power of the number N_{part} of participating nucleons, $\rho \sim N_{\mathrm{part}}^{1/3}$. The density of partons defines the value of the saturation scale, and so we expect

$$Q_{\mathrm{s}}^2 \sim N_{\mathrm{part}}^{1/3} \,. \tag{65}$$

The gluon multiplicity is then, as we discussed above

$$\frac{dN_g}{d\eta} \sim \frac{S_A \; Q_{\mathrm{s}}^2}{\alpha_{\mathrm{s}}(Q_{\mathrm{s}}^2)} \,, \tag{66}$$

where S_A is the nuclear overlap area, determined by atomic number and the centrality of collision. Since $S_A \; Q_{\mathrm{s}}^2 \sim N_{\mathrm{part}}$ by definitions of the transverse density and area, from (66) we get

$$\frac{dN_g}{d\eta} \sim N_{\mathrm{part}} \;\; \ln N_{\mathrm{part}} \,, \tag{67}$$

which shows that the gluon multiplicity shows a logarithmic deviation from the scaling in the number of participants.

To quantify the argument, we need to explicitly evaluate the average density of partons at a given centrality. This can be done by using Glauber theory, see [41, 45] for details.

4.2. Energy dependence

Let us now turn to the discussion of energy dependence of hadron production. In semi-classical scenario, it is determined by the variation of saturation scale $Q_{\rm s}$ with Bjorken $x = Q_{\rm s}/\sqrt{s}$. This variation, in turn, is determined by the x-dependence of the gluon structure function. In the saturation approach, the gluon distribution is related to the saturation scale by Eq. (45). A good description of HERA data is obtained with saturation scale $Q_{\rm s}^2 = 1 \div 2$ GeV^2 with W-dependence ($W \equiv \sqrt{s}$ is the center-of-mass energy available in the photon–nucleon system) [54]

$$Q_{\rm s}^2 \propto W^{\lambda}\,, \tag{68}$$

where $\lambda \simeq 0.25 \div 0.3$. In spite of significant uncertainties in the determination of the gluon structure functions, perhaps even more important is the observation [54] that the HERA data exhibit scaling when plotted as a function of variable

$$\tau = \frac{Q^2}{Q_0^2}\ \left(\frac{x}{x_0}\right)^{\lambda}, \tag{69}$$

where the value of λ is again within the limits $\lambda \simeq 0.25 \div 0.3$. In high density QCD, this scaling is a consequence of the existence of dimensionful scale [26, 29]

$$Q_{\rm s}^2(x) = Q_0^2 \left(\frac{x_0}{x}\right)^{\lambda}. \tag{70}$$

Using the value of $Q_{\rm s}^2 \simeq 2.05$ GeV^2 extracted [41] at $\sqrt{s} = 130$ GeV and $\lambda = 0.25$ [54] used in [47], equation (80) leads to the following approximate formula for the energy dependence of charged multiplicity in central Au–Au collisions:

$$\left\langle \frac{2}{N_{\rm part}}\ \frac{dN_{\rm ch}}{d\eta} \right\rangle_{\eta<1} \approx\ 0.87\ \left(\frac{\sqrt{s}\ ({\rm GeV})}{130}\right)^{0.25} \times \left[3.93 + 0.25\ \ln\left(\frac{\sqrt{s}\ ({\rm GeV})}{130}\right)\right]. \tag{71}$$

At $\sqrt{s} = 130$ GeV, we estimate from Eq.(71) $2/N_{\rm part}\ dN_{\rm ch}/d\eta\ |_{\eta<1} = 3.42 \pm 0.15$, to be compared to the average experimental value of 3.37 ± 0.12 [50–53]. At $\sqrt{s} = 200$ GeV, one gets 3.91 ± 0.15, to be compared to the PHOBOS value [52] of 3.78 ± 0.25. Finally, at $\sqrt{s} = 56$ GeV, we find 2.62 ± 0.15, to be compared to [52] 2.47 ± 0.25. It is interesting to note that formula (71), when extrapolated to very high energies, predicts for the LHC energy a value substantially smaller than found in other approaches:

$$\left\langle \frac{2}{N_{\rm part}}\ \frac{dN_{\rm ch}}{d\eta} \right\rangle_{\eta<1} = 10.8 \pm 0.5\,, \quad \sqrt{s} = 5500\ {\rm GeV}, \tag{72}$$

corresponding only to a factor of 2.8 increase in multiplicity between the RHIC energy of $\sqrt{s} = 200$ GeV and the LHC energy of $\sqrt{s} = 5500$ GeV (numerical calculations show that when normalized to the number of participants, the multiplicity in central Au–Au and Pb–Pb systems is almost identical).

4.3. Radiating the glue

Let us now proceed to the quantitative calculation of the (pseudo-) rapidity and centrality dependences [55]. We need to evaluate the leading tree diagram describing emission of gluons on the classical level. Let us introduce the unintegrated gluon distribution $\varphi_A(x, k_\mathrm{t}^2)$ which describes the probability to find a gluon with a given x and transverse momentum k_t inside the nucleus A. As follows from this definition, the unintegrated distribution is related to the gluon structure function by

$$xG_A(x, p_\mathrm{t}^2) = \int^{p_\mathrm{t}^2} dk_\mathrm{t}^2 \; \varphi_A(x, k_\mathrm{t}^2)\,, \tag{73}$$

when $p_\mathrm{t}^2 > Q_\mathrm{s}^2$, the unintegrated distribution corresponding to the bremsstrahlung radiation spectrum is

$$\varphi_A(x, k_\mathrm{t}^2) \sim \frac{\alpha_\mathrm{s}}{\pi} \frac{1}{k_\mathrm{t}^2}\,. \tag{74}$$

In the saturation region, the gluon structure function is given by (46); the corresponding unintegrated gluon distribution has only logarithmic dependence on the transverse momentum:

$$\varphi_A(x, k_\mathrm{t}^2) \sim \frac{S_A}{\alpha_\mathrm{s}}\,, \quad k_\mathrm{t}^2 \le Q_\mathrm{s}^2\,, \tag{75}$$

where S_A is the nuclear overlap area, determined by the atomic numbers of the colliding nuclei and by centrality of the collision.

The differential cross section of gluon production in a AA collision can now be written down as [26, 48]

$$E\frac{d\sigma}{d^3p} = \frac{4\pi N_\mathrm{c}}{N_\mathrm{c}^2 - 1} \frac{1}{p_\mathrm{t}^2} \int dk_\mathrm{t}^2 \; \alpha_\mathrm{s} \; \varphi_A(x_1, k_\mathrm{t}^2) \; \varphi_A(x_2, (p-k)_\mathrm{t}^2)\,, \tag{76}$$

where $x_{1,2} = (p_\mathrm{t}/\sqrt{s}) \exp(\pm\eta)$, with η the (pseudo)rapidity of the produced gluon; the running coupling α_s has to be evaluated at the scale

$Q^2 = \max\{k_{\rm t}^2, (p-k)_{\rm t}^2\}$. The rapidity density is then evaluated from (76) according to

$$\frac{dN}{dy} = \frac{1}{\sigma_{AA}} \int d^2p_{\rm t} \left(E \frac{d\sigma}{d^3p} \right), \tag{77}$$

where σ_{AA} is the inelastic cross section of nucleus–nucleus interaction.

Since the rapidity y and Bjorken variable are related by $\ln 1/x = y$, the x-dependence of the gluon structure function translates into the following dependence of the saturation scale $Q_{\rm s}^2$ on rapidity:

$$Q_{\rm s}^2(s; \pm y) = Q_{\rm s}^2(s; y=0) \, \exp(\pm \lambda y) \, . \tag{78}$$

As it follows from (78), the increase of rapidity at a fixed $W \equiv \sqrt{s}$ moves the wave function of one of the colliding nuclei deeper into the saturation region, while leading to a smaller gluon density in the other, which as a result can be pushed out of the saturation domain. Therefore, depending on the value of rapidity, the integration over the transverse momentum in Eqs. (76), (77) can be split in two regions: *(i)* the region $\Lambda_{\rm QCD} < k_{\rm t} < Q_{\rm s,min}$ in which the wave functions are both in the saturation domain; and *(ii)* the region $\Lambda \ll Q_{\rm s,min} < k_{\rm t} < Q_{\rm s,max}$ in which the wave function of one of the nuclei is in the saturation region and the other one is not. Of course, there is also the region of $k_{\rm t} > Q_{\rm s,max}$, which is governed by the usual perturbative dynamics, but our assumption here is that the rôle of these genuine hard processes in the bulk of gluon production is relatively small; in the saturation scenario, these processes represent quantum fluctuations above the classical background. It is worth commenting that in the conventional mini-jet picture, this classical background is absent, and the multi-particle production is dominated by perturbative processes. This is the main physical difference between the two approaches; for the production of particles with $p_{\rm t} \gg Q_{\rm s}$ they lead to identical results.

To perform the calculation according to (77), (76) away from $y = 0$ we need also to specify the behavior of the gluon structure function at large Bjorken x (and out of the saturation region). At $x \to 1$, this behavior is governed by the QCD counting rules, $xG(x) \sim (1-x)^4$, so we adopt the following conventional form: $xG(x) \sim x^{-\lambda} \, (1-x)^4$.

We have now everything at hand to perform the integration over transverse momentum in (77), (76); the result is the following [55]:

$$\begin{aligned} \frac{dN}{dy} \; &= \; \text{const.} \; S_A \; Q_{\rm s,min}^2 \; \ln \left(\frac{Q_{\rm s,min}^2}{\Lambda_{\rm QCD}^2} \right) \\ &\times \left[1 + \frac{1}{2} \; \ln \left(\frac{Q_{\rm s,max}^2}{Q_{\rm s,min}^2} \right) \; \left(1 - \frac{Q_{\rm s,max}}{\sqrt{s}} e^{|y|} \right)^4 \right], \end{aligned} \tag{79}$$

where the constant is energy–independent, S_A is the nuclear overlap area, $Q_{\rm s}^2 \equiv Q_{\rm s}^2(s; y=0)$, and $Q_{\rm s,min(max)}$ are defined as the smaller (larger) values of (78); at $y=0$, $Q_{\rm s,min}^2 = Q_{\rm s,max}^2 = Q_{\rm s}^2(s) = Q_{\rm s}^2(s_0) \ \times (s/s_0)^{\lambda/2}$. The first term in the brackets in (79) originates from the region in which both nuclear wave functions are in the saturation regime; this corresponds to the familiar $\sim (1/\alpha_{\rm s})\, Q_{\rm s}^2 R_A^2$ term in the gluon multiplicity. The second term comes from the region in which only one of the wave functions is in the saturation region. The coefficient $1/2$ in front of the second term in square brackets comes from $k_{\rm t}$ ordering of gluon momenta in evaluation of the integral of Eq. (76).

The formula (79) has been derived using the form (75) for the unintegrated gluon distributions. We have checked numerically that the use of more sophisticated functional form of φ_A taken from the saturation model of Golec-Biernat and Wüsthoff [54] in Eq. (76) affects the results only at the level of about 3%.

Since $S_A Q_{\rm s}^2 \sim N_{\rm part}$ (recall that $Q_{\rm s}^2 \gg \Lambda_{\rm QCD}^2$ is defined as the density of partons in the transverse plane, which is proportional to the density of participants), we can re-write (79) in the following final form [55]

$$\frac{dN}{dy} \ = \ c\ N_{\rm part}\ \left(\frac{s}{s_0}\right)^{\frac{\lambda}{2}}\ e^{-\lambda|y|}\ \left[\ln\left(\frac{Q_{\rm s}^2}{\Lambda_{\rm QCD}^2}\right) - \lambda|y|\right] \times \left[1 + \lambda|y|\left(1 - \frac{Q_{\rm s}}{\sqrt{s}}\, e^{(1+\lambda/2)|y|}\right)^4\right], \tag{80}$$

with $Q_{\rm s}^2(s) = Q_{\rm s}^2(s_0)\ (s/s_0)^{\lambda/2}$. This formula expresses the predictions of high density QCD for the energy, centrality, rapidity, and atomic number dependences of hadron multiplicities in nuclear collisions in terms of a single scaling function. Once the energy-independent constant $c \sim 1$ and $Q_{\rm s}^2(s_0)$ are determined at some energy s_0, Eq. (80) contains no free parameters. At $y=0$ the expression (79) coincides exactly with the one derived in [41], and extends it to describe the rapidity and energy dependences.

4.4. Converting gluons into hadrons

The distribution (80) refers to the radiated gluons, while what is measured in experiment is, of course, the distribution of final hadrons. We thus have to make an assumption about the transformation of gluons into hadrons. The gluon mini-jets are produced with a certain virtuality, which changes as the system evolves; the distribution in rapidity is thus not preserved. However, in the analysis of jet structure it has been found that the *angle* of the produced gluon is remembered by the resulting hadrons; this property of "local parton–hadron duality" (see [49] and references therein) is

natural if one assumes that the hadronization is a soft process which cannot change the direction of the emitted radiation. Instead of the distribution in the angle θ, it is more convenient to use the distribution in pseudo–rapidity $\eta = -\ln\tan(\theta/2)$. Therefore, before we can compare (79) to the data, we have to convert the rapidity distribution (80) into the gluon distribution in pseudo-rapidity. We will then assume that the gluon and hadron distributions are dual to each other in the pseudo-rapidity space; the conversion from the rapidity y to pseudo-rapidity η is accomplished with the help of Jacobian, see [47] for details.

The results for the Au–Au collisions at $\sqrt{s} = 130$ GeV are presented in Figs 4 and 5. One can see that both the centrality dependence and the rapidity dependence of the $\sqrt{s} = 130$ GeV PHOBOS data are well reproduced below $\eta \simeq \pm 4$. The predictions of this approach were also successful at other RHIC energies, from $\sqrt{s} = 20$ GeV to $\sqrt{s} = 200$ GeV.

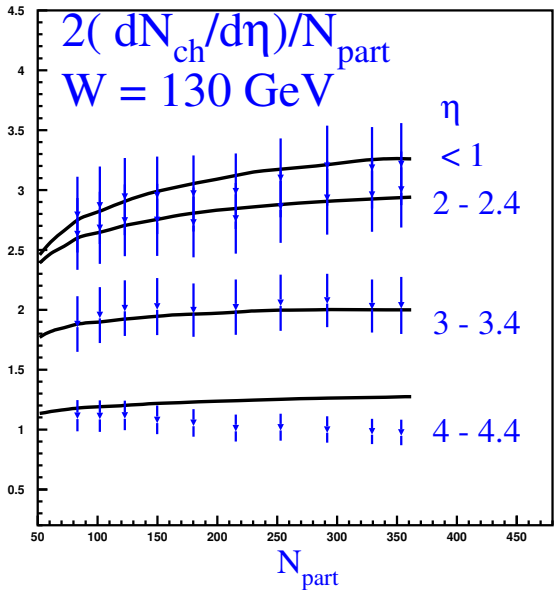

Fig. 4. Centrality dependence of charged hadron production per participant at different pseudo-rapidity η intervals in Au–Au collisions at $\sqrt{s} = 130$ GeV; from [55], the data are from [52].

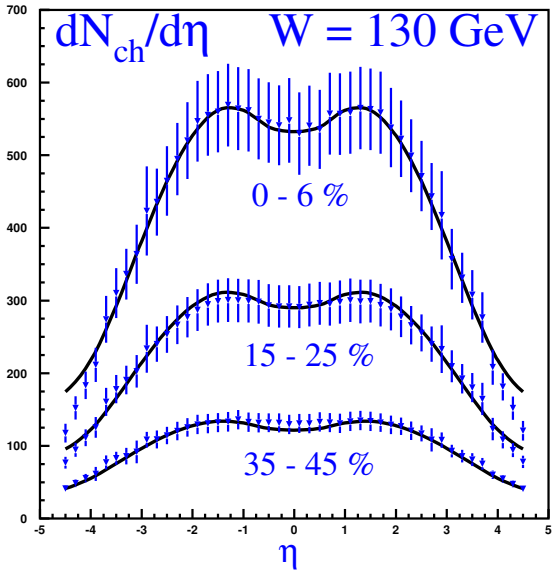

Fig. 5. Pseudo-rapidity dependence of charged hadron production at different cuts on centrality in Au–Au collisions at $\sqrt{s} = 130$ GeV; from [55], the data are from [52].

5. Summary and outlook

In these lectures, we have discussed the general ideas underlying the semi-classical approach to high energy interactions in QCD. We have also considered in detail just one application of these ideas: namely, the evaluation of the multiplicity distributions in high energy nuclear collisions. Because of the lack of space, many other directions in this rapidly developing field have not been covered. Among them are such important developments as the first-principle numerical lattice approach to the evolution of classical gauge fields, the recent work on the non-linear evolution equation at small x, and the manifestations of non-linear evolution in hard processed at small x; I refer the reader to review articles [1–4] as well as to the other lectures in this volume for gaining a broader prospective.

I am grateful to Michał Praszałowicz and his colleagues for inviting me to this excellent School. I also wish to thank my collaborators — Yu. Kovchegov, E. Levin, L. McLerran, M. Nardi, K. Tuchin and R. Venugopalan for sharing their insights with me. The work was supported by the U.S. Department of Energy under Contract No. DE-AC02-98CH10886.

REFERENCES

[1] L. McLerran, hep-ph/0311028.

[2] E. Iancu, R. Venugopalan, hep-ph/0303204.

[3] J. Jalilian-Marian, Yu.V. Kovchegov, *Prog. Part. Nucl. Phys.* **56**, 104 (2006) [hep-ph/0505052].

[4] D.E. Kharzeev, J. Raufeisen, nucl-th/0206073.

[5] R.D. Field, *Applications of Perturbative QCD*, Addison-Wesley, New York, USA 1989.

[6] R.K. Ellis, W.J. Stirling, B.R. Webber, *QCD and Collider Physics*, Cambridge University Press, Cambridge, UK 1996.

[7] T. Muta, *Foundations of Quantum Chromodynamics*, World Scientific, Singapore 1987.

[8] L.D. Landau, I.Ya. Pomeranchuk, *Dokl. Akad. Nauk Ser. Fiz.* **102**, 489 (1955); also published in *The Collected Papers of L.D. Landau*, ed. D. Ter Haar, Pergamon Press, 1965, pp. 654–658.

[9] V.N. Gribov, *Eur. Phys. J.* **C10**, 71 (1999) [hep-ph/9807224].

[10] Y.L. Dokshitzer, D.E. Kharzeev, *Annu. Rev. Nucl. Part. Sci.* **54**, 487 (2004) [hep-ph/0404216].

[11] D.J. Gross, F. Wilczek, *Phys. Rev. Lett.* **30**, 1343 (1973); H.D. Politzer, *Phys. Rev. Lett.* **30**, 1346 (1973).

[12] N.K. Nielsen, *Am. J. Phys.* **49**, 1171 (1981).

[13] L.D. Landau, E.M. Lifshits, *Quantum Mechanics: Nonrelativistic Theory, Landau-Lifshits Physics Course*, Vol. 3, Pergamon Press, Oxford, UK 1965.

[14] S. Bethke, *J. Phys. G* **26**, R27 (2000) [hep-ex/0004021].

[15] K. Wilson, *Phys. Rev.* **D10**, 2445 (1974).

[16] S.L. Adler, *Phys. Rev.* **177**, 2426 (1969); J.S. Bell, R. Jackiw, *Nuovo Cim.* **A60**, 47 (1969).

[17] T. Schäfer, E.V. Shuryak, *Rev. Mod. Phys.* **70**, 323 (1998) [hep-ph/9610451].

[18] H. Forkel, hep-ph/0009136.

[19] R.D. Peccei, H.R. Quinn, *Phys. Rev. Lett.* **38**, 1440 (1977); *Phys. Rev.* **D16**, 1791 (1977); F. Wilczek, *Phys. Rev. Lett.* **40**, 279 (1978); S. Weinberg, *Phys. Rev. Lett.* **40**, 223 (1978).

[20] T.D. Lee, G.C. Wick, *Phys. Rev.* **D9**, 2291 (1974).

[21] K. Rajagopal, F. Wilczek, hep-ph/0011333.

[22] F. Karsch, hep-ph/0610024.

[23] D.E. Kharzeev, R.D. Pisarski, M.H. Tytgat, *Phys. Rev. Lett.* **81**, 512 (1998) [hep-ph/9804221]; D.E. Kharzeev, R.D. Pisarski, *Phys. Rev.* **D61**, 111901 (2000) [hep-ph/9906401]; D. Kharzeev, *Phys. Lett.* **B633**, 260 (2006) [hep-ph/0406125].

[24] I.V. Selyuzhenkov (STAR Collaboration), *Rom. Rep. Phys.* **58**, 049 (2006) [nucl-ex/0510069].

[25] D.E. Kharzeev, *Nucl. Phys.* **A699**, 95 (2002) [nucl-th/0107033].

[26] L.V. Gribov, E.M. Levin, M.G. Ryskin, *Phys. Rep.* **100**, 1 (1983).

[27] A.H. Mueller, J.-W. Qiu, *Nucl. Phys.* **B268**, 427 (1986).

[28] J.P. Blaizot, A.H. Mueller, *Nucl. Phys.* **B289**, 847 (1987).

[29] L.D. McLerran, R. Venugopalan, *Phys. Rev.* **D49**, 2233 (1994); **D49**, 3352 (1994).

[30] I. Iancu, A. Leonidov, L. McLerran, hep-ph/0202270.

[31] A.H. Mueller, hep-ph/0111244.

[32] D. Kharzeev, Yu. Kovchegov, E. Levin, *Nucl. Phys.* **A690**, 621 (2001).

[33] M. Nowak, E. Shuryak, I. Zahed, *Phys. Rev.* **D64**, 034008 (2001).

[34] D. Kharzeev, Yu. Kovchegov, E. Levin, *Nucl. Phys.* **A699**, 745 (2002).

[35] V.B. Berestetskii, E.M. Lifshitz, L.P. Pitaevskii, *Quantum Electrodynamics*, Pergamon Press, Oxford New York 1982.

[36] D. Kharzeev, E. Levin, L. McLerran, *Nucl. Phys.* **A748**, 627 (2005) [hep-ph/0403271].

[37] H. Pagels, E. Tomboulis, *Nucl. Phys.* **B143**, 485 (1978).

[38] A.A. Migdal, M.A. Shifman, *Phys. Lett.* **B114**, 445 (1982).

[39] P. Castorina, M. Consoli, *Phys. Rev.* **D35**, 3249 (1987).

[40] D. Kharzeev, E. Levin, K. Tuchin, *Phys. Rev.* **D70**, 054005 (2004) [hep-ph/0403152].

[41] D. Kharzeev, M. Nardi, *Phys. Lett.* **B507**, 121 (2001).

[42] D. Kharzeev, K. Tuchin, *Nucl. Phys.* **A753**, 316 (2005) [hep-ph/0501234]; D. Kharzeev, E. Levin, K. Tuchin, hep-ph/0602063.

[43] D. Kharzeev, A. Krasnitz, R. Venugopalan, *Phys. Lett.* **B545**, 298 (2002) [hep-ph/0109253].

[44] T. Lappi, L. McLerran, *Nucl. Phys.* **A772**, 200 (2006) [hep-ph/0602189]; T. Lappi, hep-ph/0606207.

[45] D. Kharzeev, C. Lourenço, M. Nardi, H. Satz, *Z. Phys.* **C74**, 307 (1997).

[46] C. De Jager, H. De Vries, C. De Vries, *At. Data Nucl. Data Tables* **14**, 479 (1974).

[47] D. Kharzeev, E. Levin, *Nucl. Phys.* **B578**, 351 (2000).

[48] M. Gyulassy, L. McLerran, *Phys. Rev.* **C56**, 2219 (1997).

[49] Yu.L. Dokshitzer, hep-ph/9812252.

[50] K. Adcox *et al.* (PHENIX Collaboration), *Phys. Rev. Lett.* **86**, 3500 (2001); *Phys. Rev. Lett.* **87**, 052301 (2001); A. Milov *et al.* (PHENIX Collaboration), *Nucl. Phys.* **A698**, 171 (2002) nucl-ex/0107006.

[51] C. Adler *et al.* (STAR Collaboration), *Phys. Rev. Lett.* **87**, 112303 (2001); *Phys. Rev. Lett.* **87**, 082301 (2001).

[52] B. Back *et al.* (PHOBOS Collaboration), *Phys. Rev. Lett.* **85**, 3100 (2000); *Phys. Rev. Lett.* **87**, 102303 (2001); *Phys. Rev.* **C65**, 031901 (2002) [nucl-ex/0105011]; *Phys. Rev. Lett.* **88**, 022302 (2002) [nucl-ex/0108009].

[53] I.G. Bearden *et al.* (BRAHMS Collaboration), *Phys. Rev. Lett.* **87**, 112305 (2001); nucl-ex/0102011; *Phys. Lett.* **B523**, 227 (2001) [nucl-ex/0108016].

[54] K. Golec-Biernat, M. Wüsthoff, *Phys. Rev.* **D59**, 014017 (1999); *Phys. Rev.* **D60**, 114023 (1999); A. Stasto, K. Golec-Biernat, J. Kwiecinski, *Phys. Rev. Lett.* **86**, 596 (2001).

[55] D. Kharzeev, E. Levin, *Phys. Lett.* **B523**, 79 (2001).